Displays 47 (2017) 2–11

Contents lists available at ScienceDirect

Displays

journal homepage: www.elsevier.com/locate/displa

Comparative study on the effect of Parameter Mapping Sonification on perceived instabilities, efficiency, and accuracy in real-time interactive exploration of noisy data streams ☆

David Poirier-Quinot [a,*], Gaetan Parseihian [b], Brian F.G. Katz [c]

[a] Airbus D&S, Elancourt and LIMSI-CNRS, Orsay, France
[b] LMA-CNRS-UPR 7051, Aix-Marseille Univ., Centrale Marseille, France
[c] LIMSI-CNRS, Orsay, France

ARTICLE INFO

Article history:
Received 5 August 2015
Received in revised form 29 February 2016
Accepted 6 May 2016
Available online 7 May 2016

Keywords:
Parameter mapping sonification
Real-time interaction
Noise perception

ABSTRACT

This paper presents a comparative study on common Parameter Mapping Sonifications (PMSons) designed to reduce the perception of instabilities during the real-time interactive exploration of noisy data streams. The objective of this study is to evaluate the capacity of these PMSons in reducing the perceived fluctuations while preserving both efficiency and accuracy of participants' estimations during the exploration task. Based on the real application of beacon localization for rescue operations, an abstraction of the task was developed which simulates the basic concepts involved, i.e. the estimation of local maxima during the exploration of a 1D data topography. Three different PMSons were selected, based on pitch, pitch averaged over time, and tempo, evaluated for three different noise levels applied to the data. Subjects explored the auditory graph using a pen tablet to define their auditory viewpoint (i.e. position) on the topography. Evaluations were based on subjects' ability to quickly appraise the underlying data topography along with aesthetic considerations regarding the impact of noise on the exploration task. Results showed that both tempo and pitch averaged PMSon reduced the perceived instabilities compared to pitch, while tempo preserved the response time of the sonification feedback.

1. Introduction

Sonification is defined as the embedding of information into audio streams, regarded as a sound-based equivalent of visualization [1]. Its use in Human Computer Interfaces (HCI) spread as it became understood how sonification could be used to supplement visual displays or for parallel task monitoring when visual attention was already focused elsewhere [2,3]. Subsequently, researchers in the field of auditory display have explored and defined various use cases and applications that attempt to make full use of the various strengths of the human auditory system [4,5].

Detailed in Section 2, the considered application context is related to search and rescue operations, supposing cellphone localization based on an audio guidance device. In essence, the search process consists in the exploration of a 1D data topography, where said exploration is based on a sonified line graph. The term topography here designs a set of data values distributed on a line (1D topography) or a plane (2D topography). Sonified line graphs are a sub-category of auditory graphs: equivalent to visual plots, graphs, and charts for the audio modality, introduced by Mansur et al. as "sound graphs" in 1985 [6]. The application field for auditory graphs has long been the design of assistive devices for the visually impaired [7–9], typically exploited and evaluated through point estimation [10], trend assessment [11], or dataset comparisons tasks [12]. Sonified graphs were progressively exploited for sighted user interfaces as comparative studies proved their worth for high-level data exploration to, for example, effortlessly spot subtle changes in complex repeated sound patterns [4,13].

Most auditory graph applications are based on Parameter Mapping Sonification (PMSon), a sonification technique that assumes the mapping of data values onto sound parameters (e.g. pitch, tempo, spatial position, etc.) [14]. Investigations on PMSon often evaluate the impact of the designed mapping on the subjective perception of the data [15] or the quality and amount of information that can be "displayed" with a given interface [16–18].

The considered exploration task supposes an interactive exploration, as opposed to a passive listening based on an automatic

☆ This paper was recommended for publication by Richard H.Y. So.

* Corresponding author.
E-mail addresses: davipoir@limsi.fr (D. Poirier-Quinot), parseihian@lma.cnrs-mrs.fr (G. Parseihian), brian.katz@limsi.fr (B.F.G. Katz).

http://dx.doi.org/10.1016/j.displa.2016.05.001
0141-9382/

scrolling of the auditory viewpoint through the data stream [12]. In most designs, this interaction is carried out through 1D, 2D, or 3D interfaces depending on the dimension of the explored topography, allowing participants to focus the sonification, and thus their attention, on points or regions of the graph [19,20].

1.1. Motivation

Due to the application context, the topographies examined in the current study are based on data containing a certain degree of noise, intrinsic to their real-time acquisition. This raises the question of the suitability of traditional PMSon approaches as direct sonification of noisy data could lead to serious fatigue issues caused by prolonged listening to continuously *jittery* sonifications. Few studies have tackled the sonification of real-time data streams, and fewer still the issues related to noisy data. Noise is typically removed upstream of the sonification, e.g. through signal processing algorithms [21]. For real-time applications, such processing is likely to increase the system latency and thus impact on the perceived sonification feedback reactivity (which depends on user's exploration speed relative to said system latency).

1.2. Contributions

This paper attempts to explore the effect of noise on the exploration and understanding of a sonified 1D data topography. It is similar to two previous studies addressing the impact of different sonification mappings on the general shape perception or the maximum value localization of 1D topographies [19,22]. In both studies, as with the 2D topography exploration in [23], the *pitch* of a sound was exploited to reflect local values of the topography. This mapping is generally acknowledged as a standard for basic auditory graph design [24]. For noisy data, such a traditional pitch-based PMSon would result in continuously jittering tones. Data smoothing, through the use of a running average, could be employed to reduce the jitter effect at the cost of increased latency as a function of the averaging window length. Another possible way is to use a *tempo*-based PMSon. Tempo can be seen as a "psycho-acoustic running average" (see Section 3), reducing the perceived data instabilities while preserving the HCI's response time. Tempo PMSons have previously been employed in auditory [19] and cross-modal audio-haptic interfaces [25], yet not in the context of noisy data streams.

The experiment presented in this paper is designed to explore the reduction of noise perception in sonification, comparing a pitch-based PMSon coupled with a running average and a tempo-based PMSon. The effect of these two PMSon will be compared to the effect of a traditional pitch-based PMSon. The objective of this study is to evaluate the capacity of the Pitch-Averaged and Tempo based PMSons to reduce the perceived acquisition noise while preserving both efficiency and accuracy of users' estimations during a real-time, interactive exploration task.

1.3. Organization

The remainder of this paper is organized as follows. Section 2 presents the application context. Section 3 arguments the choice of specific PMSon for noisy data sonification. Section 4 details the experimental design: task abstraction, PMSon, input data, and topography design. Section 5 describes the experimental method: subjects, stimuli, apparatus, and procedure. Finally, Sections 6 and 7 present the result and the discussion while Section 8 exposes the conclusion of this paper.

2. Context

The present study is a results of reflections on the design of an audio device used to localize victims of natural disasters. Similar to avalanche transceivers [26], the localization process relies on victims carrying a cellphone that will behave as a Radio Frequency (RF) beacon [27]. The audio device is composed of a directional antenna that feeds RF power measurements to a sonification algorithm. Operation is based on the fact that an increase of the received power occurs as the directional antenna is steered towards the RF beacon. Such a device is generally referred to as a RF Direction Finder (DF). In addition to direction variations, the magnitude of the electromagnetic field will vary as a function of DF distance to the emitting source. As such, instantaneous absolute values have little meaning. A comprehensive presentation of visual DF implementation in the context of rescue operations can be found in [28], while a virtual prototype of the considered audio

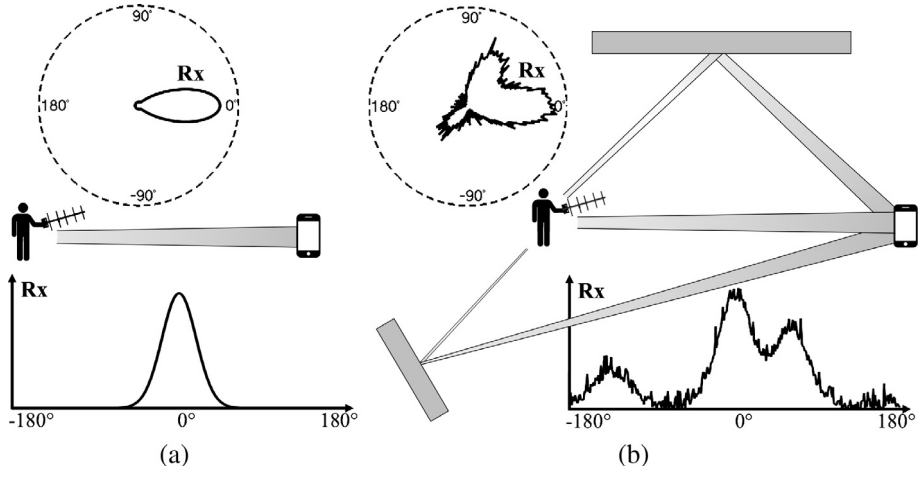

Fig. 1. Illustration of two different propagation scenarios and their impact on direction of arrival estimation by a DF user. The polar plot represents the received signal as a function of DF orientation by the user with the RF beacon at 0°. (a) Simple propagation scenario; the only signal that reaches the DF corresponds to the direct path towards the RF beacon. The DF user observes a single maximum in the received signal strength. (b) Propagation scenario in a more complex environment (e.g. urban area); multiple signals reach the DF due to reflections of the original signal emitted by the RF beacon on elements of the environment. Here, the DF user would have to identify left and right local maxima as reflections and focus on the global maximum of received signal strength, assuming it corresponds to the direct path towards the RF beacon. The measurement noise intrinsic to the acquisition is also represented.

DF has been previously presented in [29,30]. The interface of the considered DF design employs sonification in order to propose a hands and eyes-free solution for search and rescue operations.

Equipped with the DF, a rescuer's principle task in ideal conditions is to estimate the direction in which the RF signal is stronger whilst manually steering the directional antenna, as illustrated in Fig. 1(a). Actual search conditions such as urban area operations will involve multiple propagation paths from the RF beacon to the DF antenna. Fig. 1(b) illustrates the apparition of local RF power maxima induced by reflective obstacles. While they can interfere with the search process, these local maxima represent valuable information for a user able to interpret them in the context of local surroundings. Actual conditions will also involve the presence of noise in the measured RF signal power as indicated in Fig. 1(b). Supposing a PMSon-based HCI, the task is therefore to explore an auditory graph where the DF user needs to listen and compare fluctuating sound parameter values.

3. Sonification of noisy data

Preliminary tests prior to this study were conducted on a Pitch-based PMSon of the received RF power. While the design produced acceptable performance, noise induced instabilities on the pitch were reported as tiring by subjects exposed to prolonged listening. In the current study, the basic Pitch PMSon is compared to two other sonifications designed to reduce noise perception. The first implements a *running average* applied prior to the Pitch PMSon, adjusted (see Section 4.3.2) to remove most of the noise component with a minimum impact on general system latency. The second is based on *tempo*, more precisely on variations of the Inter-Onset Interval (IOI) between sound bursts as a function of DF power measurements, a sonification design often referred to as the "Geiger counter metaphor".

Based on psycho-acoustic considerations, the IOI-based PMSon can be seen as a natural equivalent of the running average. As emphasized in most perception models [31,32], tempo perception is based on a semi-conscious evaluation of burst occurrences over time intervals. Compared to pitch, this could suggest that listener's attention will more readily ignore noise-related tempo fluctuations or irregularities and will be able to focus more on averaged estimations. Compared to computational averaging, the length of these time intervals depends on the IOI duration, decreasing as the tempo increases. This observation can be seen as a corollary of Weber's law [33] on Just Noticeable Differences (JND) of tempo variations which describes humans ability to detect temporal variations as increasing when the IOI decreases. Such an adaptive dynamic of estimation and precision could offer an advantage for the considered application.

PMSon designs will be assessed according to (1) speed and precision of subjects' estimation of the global maximum position and (2) precision of subjects' estimation of local maxima positions and relative amplitudes, for different noise levels and topography difficulty.

4. Experimental design

This section provides implementation details of the task abstraction for the current experiment, data input, and sonification mappings.

4.1. Task abstraction

The real rescue search task can be seen as a spherical topography exploration, where the DF user has to find the direction of arrival of the strongest RF signal. As seen in Fig. 1, this task can be reduced to the exploration of a 1D topography if the DF user only focuses on azimuthal estimation (e.g. at distances far from the RF beacon relative to any height information). In order to ascertain condition repeatability across subjects, the abstracted 1D exploration task is based on pre-recorded DF inputs. To simplify the user interface, the exploration is carried out on a pen tablet: simulated DF antenna orientation is mapped to pen position on the tablet's horizontal axis. In sliding the pen across the tablet, subjects will hear the sound parameter variations corresponding to 0–360° DF power measurements (see Section 4.2).

Note that this abstraction may slightly affect the ecological validity of the results regarding the original task which is fundamentally an unconstrained angular exploration. The abstraction of the task to a linear exploration constrained to the 20 cm tablet width, compared to the angular 2π-times-arm-length arc, is likely to increase the exploration speed at the expense of the estimation accuracy and possible border effects at the tablet edges. As such, this study is constructed more as a comparative evaluation of the three PMSon designs and not an absolute measure of the expected results in the real search condition.

4.2. Input signal

The topographies used as PMSon inputs were based on measurements issued from an actual DF prototype, composed of a Yagi-Uda directional antenna of aperture 60°, attuned to a RF beacon emitting electromagnetic bursts at 900 MHz. Three different scenarios were considered, corresponding to different radio propagation conditions between RF beacon and DF antenna. Scenario difficulty ranged from simple to hard regarding the exploration task, composed of one to three local maxima. While scenarios 1 and 2 were based on actual measurements, the third was simulated to represent a worst case scenario in order to test the PMSons design limits in critical conditions.

Scenario C_1 – simple: outdoor, flat field, nearest RF reflective surface at approximately 50 m from both DF and RF beacon; DF at 30 m from RF beacon; 1 global maximum.
Scenario C_2 – medium: indoor, research facility, DF at approximately 30 m from RF beacon; DF and RF beacon in different rooms with 2 walls in-between; 1 global maximum, 1 additional local maximum.
Scenario C_3 – hard: simulated worst case scenario, crowded urban area, DF at approximately 30 m from RF beacon in different streets surrounded by buildings; 1 global maximum, 2 additional local maxima.

DF measurements of Root Mean Square (RMS) received RF power values were recorded for 8 different azimuthal orientations of the directional antenna at a fixed position. 100 RMS values were recorded every 45°, at a sample rate of 50 Hz, from 0° to 315°, with 0° orientation corresponding to the directional antenna pointing directly towards the RF beacon. Each RMS measurement was calculated from 512 instantaneous power values sampled at 100 MHz. The 45° measurement grid step was inferred from the spatial diversity of the C_3 scenario as observed with the 60° aperture of the antenna, judged small enough not to miss meaningful local maxima in the considered scenarios. The final basic topographies for scenarios C_1 and C_2 were obtained based on a second order spline interpolation between the 8 directional values obtained after averaging each set of 100 RMS values. The third topography was derived from a geometry-based simulation [34] in a crowded urban environment. The three resulting 0–360° topographies are shown in Fig. 2, unwrapped on a normalized linear scale.

Three conditions were defined regarding RMS measurement noise levels: **noiseless** N_0, **noisy** N_1, and **very noisy** N_2. The "noisy"

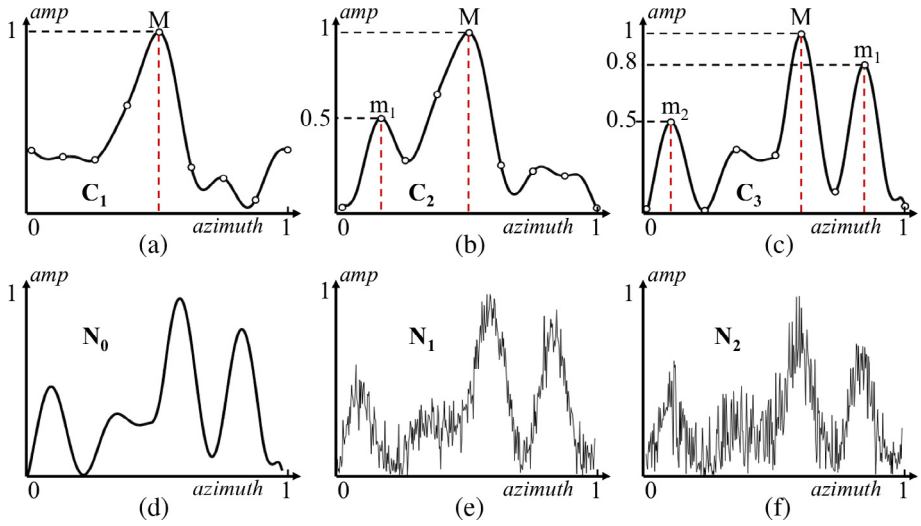

Fig. 2. Illustration of the three data topographies and noise levels. (a–b–c) Normalized plots of the received signal power as a function of antenna orientation (azimuth) for the three scenarios simple (C_1), medium (C_2), and hard (C_3) from left to right. The (○) represent averaged values over 100 measured RMS. (d–e–f) Normalized plots illustrating the three noise level conditions noiseless (N_0), noisy (N_1) and very noisy (N_2) as applied to topography C_3. Topographies were re-normalized in amplitude after the noise addition, prior to the sonification. Noise variances were slightly augmented to result in $0.8e^{-2}$ (N_1) and $3e^{-2}$ (N_2) after normalization.

N_1 condition was derived from actual RF measurements obtained in propagation conditions of scenario C_2. 100 RMS values were recorded every 45°, at the nominal audio DF sampling rate of 50 Hz. After removing any DC component, typical noise variance and spectral density were calculated and averaged across antenna orientations. Based on these parameters, a noise model was created to alter the data upstream of the sonification. The resulting model delivers instantaneous values of a low-pass filtered white Gaussian noise of variance $0.8e^{-2}$, cutoff frequency 12 Hz, quality factor $Q = 0.7$, and gain = 1. The update rate of these values was adjusted to 50 Hz to mirror the DF audio update rate and produce data instabilities that sounded comparable to those perceived during the recording session of scenario C_2. The "very noisy" N_2 condition was based on the N_1 condition, however with a $3e^{-2}$ variance, arbitrarily defined in order to explore the limitations of the three sonification designs.

4.3. Sonification metaphor design

A given PMSon efficiency relies principally on three design choices: mapping dimension, polarity, and scale [35]. The mapping dimension defines the sound parameter to which data values are mapped. Polarity indicates if data and sound parameter variations are proportional (i.e. *positive* polarity) or inversely proportional (i.e. *negative* polarity). Finally, the scaling defines the bijection elaborated between data and sound parameter domains.

The objective comparison of sonification metaphors regarding their capacity to provide information on a data-set eventually leads to considerations of normalization across perceptive scales. Parseihian et al. in [19] designed PMSons for a similar study based on the Just Noticeable Difference (JND) approach of Grond and Berger [14]. This approach attempts to establish a one-to-one JND scale between sound parameter variations. As a result, listeners should have the same sensitivity when exploring data through each PMSon. We shall refer to this concept as "inter-PMSon iso-sensitivity". This concept also suggests the implementation of PMSon scaling functions based on perceptual linearity, providing "intra-PMSon iso-sensitivity". These sensible guidelines have been adopted for the PMSon designs in the current study in order to legitimize inter-PMSon comparison and facilitate inter-study cross-analysis.

4.3.1. Pitch (P)

Sound parameter: The pitch based PMSon P is based on the perceived frequency of a sound, here a pure tone:

$$s(t, y) = A(f_{pitch}(y_{norm}))\cos\left(2\pi f_{pitch}(y_{norm})t\right)$$

where $y_{norm} = C(x_{norm}) \in [0, 1]$ represents the normalized topography height at the pen normalized horizontal position $x_{norm} \in [0, 1]$ on the tablet, and $f_{pitch}(\cdot)$ the scaling function. The weighting coefficient $A(\cdot)$ is applied to the amplitude of the sine wave to ensure a constant perceived loudness across all frequencies, after the isophonic curve from Standard ISO 226 [36].

Polarity: positive (pitch increases as data values increase).

Scaling: The scaling function $f_{pitch}(\cdot)$ is logarithmic to match human perception (intra-PMSon iso-sensitivity):

$$f_{pitch}(y_{norm}) = f_{min}2^{y_{norm}n_{oct}}$$

with $n_{oct} = (\ln 2)^{-1}\ln(f_{max}/f_{min})$ the number of octaves covered by the sonification and f_{min} and f_{max} the extreme frequency values (also designed as ambitus). The scaling function spans over 2.66 octaves, from 300 to 1900 Hz, both in accordance with the [62 Hz, 2637 Hz] range recommended in [37] and equal to the number of JNDs of the IOI scaling function (inter-PMSon iso-sensitivity). Based on evaluations of pitch difference limens as a function of frequency in [38], $f_{pitch}(\cdot)$ applied between these ambitus corresponds to approximately 560 JNDs.

4.3.2. Pitch Averaged (PA)

Exact same mapping, scaling, and polarity as with PMSon P, with the addition of a running average RMS applied over $n = 25$ samples (i.e. 0.5 s of data stream at 50 Hz) upstream of the sonification:

$$y_{avg}(t_n) = \sum_{t=1}^{n-1}\frac{y_{norm}(t_n - t)}{n}$$

with t_n and t expressed in samples. This 25 samples window was carefully chosen to remove most of the perceived noise with a minimum impact on sonification latency. The running average corresponds to a sinus cardinal frequency filtering with unitary gain and first zero-crossing at 1 Hz. Supposing a noiseless topography,

Table 1
Coefficients of the polynomial function f_{IOI} that defines IOI values as a function of topography's amplitude y_{norm}. The original function was designed based on Fig. 2 of [39] which reports 560 JNDs (or Difference-Limens) between 1 and 320 cps. Values of y_{norm} 0–1 were mapped to IOI values from 1 to 320 such that: for $n \in [\![2, 560]\!]$, $f_{IOI}(y_{norm} = n/560) = u_n = u_{n-1} + \mathrm{JND}(u_{n-1})$ cps with $u_1 = 1$ cps and $\mathrm{JND}(u_{n-1})$ the value of the JND in [39] Fig. 2 for IOI$= u_{n-1}$ cps. The two 7th order interpolations were calculated based on the resulting points, the interval [0,1] was split to ensure well behaved polynomial interpolations.

y_{norm}	a_1	a_2	a_3	a_4	a_5	a_6	a_7	a_8
$[0, 0.2)$	$-5.36e^7$	$4.81e^7$	$-1.87e^7$	$4.24e^6$	$-6.40e^5$	$7.06e^4$	$-5.92e^3$	$3.23e^2$
$[0.2, 1)$	$-2.07e^3$	$9.84e^3$	$-1.99e^4$	$2.21e^4$	$-1.49e^4$	$6.09e^3$	$-1.46e^3$	$1.67e^2$

this PMSon behaves exactly like the Pitch PMSon when the pen is moved slowly across the tablet (e.g. below 0.1 cm s^{-1}) and smoothes the topography more and more as the exploration speed increases.

4.3.3. Tempo (IOI)

Sound parameter: The tempo PMSon is based on the IOI between bursts of pink noise, achieved through cycle period variations of a square wave modulation. The square wave duty cycle was fixed to 0.2 (i.e. individual burst duration = 0.2 × cycle period), with the period defined by the scaling function $f_{IOI}(\cdot)$.
Polarity: negative (IOI decreases as data values increase).
Scaling: The scaling function $f_{IOI}(\cdot)$ has been designed to provide as much intra-PMSon iso-sensitivity as possible, along with an equivalent number of JND as in PMSon *P*. Based on measured JND of temporal variations as a function of IOI in Fig. 2 of [39], $f_{IOI}(\cdot)$ is composed of two 7th order polynomial interpolations:

$$f_{IOI}(y_{norm}) = \sum_{n=1}^{8} a_n y_{norm}^{8-n}$$

which produce tempos ranging from 1 to 320 cycles per second (cps), for approximately 560 JNDs (see Table 1).

Pending a rigorous scaling methodology, inter- and intra-PMSons iso-sensitivity will be roughly assessed through result analysis. Relaxed for the task at hand, a valid inter-PMSons iso-sensitivity (initially same number of JNDs in both PMSon) would correspond to subjects being able to evaluate topography trends with equivalent accuracy with both pitch *P* & *PA* and *IOI* PMSons. A valid intra-PMSon iso-sensitivity (initially linear perception across PMSon) would correspond to subjects being able to correctly evaluate local maxima amplitudes relative to each other with a given PMSon.

5. Method

5.1. Subjects

18 subjects participated in the experiment (3 women and 15 men), aged between 24 and 61 (mean age 31 ± 9). Six were considered as expert (musicians or actively working in the audio domain), two were left-handed. Subjects were paid volunteers (10 €), none reported any hearing loss regarding the frequency range of the experimental stimuli.

5.2. Stimuli and apparatus

Subjects were equipped with a stereo open circumaural headphone (model Sennheiser HD600) and placed in front of a pen tablet with active surface dimensions 16 × 21 cm (model Wacom Intuos 3:6 × 8). The experimental session was conducted in a quiet listening room, using an interactive interface implemented using the Max programming environment,[1] running on an OSX computer connected to a RME Fireface 800 sound-card. The computer screen was used to display task instructions and feedback during both experimental and training sessions. Subjects were free to adjust the volume once at the beginning of the experiment as no PMSon was based on perceived loudness.

Stimuli were synthesized in real-time according to the PMSons defined in Section 4.3 based on the topographies defined in Section 4.2. To avoid subjects learning the 3 topographies of Fig. 2, 9 different versions of each were created through a simple circular shift, placing the main maximum at normalized positions $\{0.1, 0.2, \ldots, 0.9\}$ on the horizontal axis. PMSon ambitus, i.e. lower and upper sound parameter limits, were randomly shifted to prevent subjects from learning what each PMSon sounded like at global maxima, i.e. for $y_{norm} = 1$. The random shift was induced upstream from the noise injection by remapping y_{norm} values from $[0, 1]$ to $[0.1 + \varepsilon, 0.9 + \varepsilon]$ with ε in $[-0.1, 0.1]$.

5.3. Procedure

The chosen experimental design was a repeated measures design with 3 main factors: PMSon, topography difficulty (i.e. number of maxima), and noise level. A fourth and minor factor was the topography shift, introduced to avoid subject detection of any experimental pattern (9 different shifts). These factors, along with associated evaluation metrics concerned with task execution efficiency and strategies, are presented in Table 2.

The experiment was divided into 3 blocks of 27 trials each. Each block concerned a unique PMSon and presented 3 repetitions of the 3×3 noise level and curve difficulty conditions ($3 \times 3 \times 3 = 27$ trials). Noise and curve conditions were semi-randomly distributed within the trials such that a given noise level or curve was never met more than twice in a row. A balanced Latin-square crossover design was applied to the 3×6 subjects for the presentation order of the PMSons to avoid carryover effects during the evaluation, the 6 potential combinations evenly distributed amongst them. Topography shifts were semi-randomly applied such that the main maximum position on the horizontal axis was never repeated more than twice in a row. Three predefined training trials were added at the beginning of each block in order to familiarize subjects with the PMSon exploited in the block. After each block, subjects answered a set of 4 questions each based on a five-point Likert scale, assessing their general impressions regarding the PMSon suitability for the exploration task.

Each trial consisted of a two-phase exploration task for a given noise, topography, and shift condition. Phase 1: subjects were instructed to find the global maximum of the topography as quickly and as accurately as possible. Phase 2: subjects were instructed to thoroughly explore the same topography so as to be able to draw it afterwards. There was no time constraint for phase 2, subjects were instructed to concentrate on accuracy rather than speed. In each trial, subjects were first notified of the beginning of phase 1 with an audio-visual feedback. Subjects then had to place the pen on the tablet to start the search and validate the estimated

[1] http://cycling74.com/downloads/.

Table 2
Independent and dependent variables of the experimental protocol.

Independent variables		
Subject	18	Random variable
PMSon	3	Pitch (*P*), Pitch Av. (*PA*), *IOI*
Noise level	3	Noiseless (N_0), noisy (N_1), very noisy (N_2)
Topography (number of maxima)	3	$C_1,\ C_2,\ C_3$
Shift (circular topography shift)	9	$C_{i1}, C_{i2}, \ldots, C_{i9}$ with $i \in \{1,2,3\}$
Dependent variables		
Task execution times (phases 1 and 2)		
Main maximum estimation (phase 1)		
Topography drawing (phase 2)		
Subjective remarks and answers to PMSon-related Likert items		

maximum position through keyboard press or mouse button. A second notification immediately announced the beginning of phase 2, where subjects were free to explore the same line graph topography in the same conditions [PMSon, noise, topography, shift]. After validation (keyboard press or mouse button), they drew the perceived topography on the tablet. Drawing validation concluded phase 2 and a new trial started with phase 1, for a different noise, topography, and shift condition combination. Other than the real-time visual display of phase 2 drawing, no feedback was provided regarding subjects performance in either phase 1 or 2.

The experiment started with a training session, different from the three pre-block training trials, where subjects were introduced to the current PMSon through a similar exploration and drawing task. Subjects were free to explore a simple topography (single maximum), select one of the three noise levels and activate/deactivate the visual feedback to understand how the PMSon reacted to the topography. Each PMSon was explicitly introduced and the objectives of each task defined. Subjects naturally used their dominant hand to hold the pen during the experiment.

6. Results

This section presents quantitative and qualitative results analysis, based on metrics presented in Table 2, followed by a discussion that concerns PMSon-related performance regarding the exploration task across noise level and topography conditions. The significance of results has been assessed using a 3-way repeated measures ANalysis Of VAriance (ANOVA) with PMSon (3 levels), Noise (3 levels), and Topography (3 levels) as within subjects factors, with a *p*-value threshold of 5%, reported in Table 3. For each phase, results were averaged across the three repetitions for each subject as no significant effect of repetition ID on task execution time, precision, etc. was observed. The topography shift showed no significant impact on subjects results and was not considered in further analysis steps. Student–Newman–Keuls post hoc tests were employed to test specific effects and significance levels. For the sake of readability, interactions between experimental conditions (PMSon, Noise level, and Topography) are mentioned only when significant.

6.1. Phase 1: Search for the global maximum

In phase 1, subjects had to estimate the topographies' main maximum position as fast as possible. Reported in Fig. 3(a), the task execution time was significantly lower in both *P* and *IOI* conditions than with *PA* (means of 9.9, standard deviation of ±6.5 vs. 12.6 ± 8.4 s). Reported in Table 3, execution times increased with noise level and topography difficulty, significantly between each noise level condition (means of 9.1 ± 5.5, 10.9 ± 7.5, and 12.4 ± 8.3 sec for N_0, N_1, and N_2) and topography C_1 and C_2 compared to C_3 (means of 10.2 ± 7.1 vs. 12.0 ± 7.5 s respectively).

False detection, i.e. situations where subjects designated a secondary maximum as being the global maximum, occurred only for explorations on topography C_3. This is assumed to be due to the relatively high value of the second maximum m_1 compared to *M* (c.f. Fig. 2(c)). Fig. 3(b) indicates that *P* and *IOI* caused significantly less false detections than *PA* (means of 1.9% and 3.7% vs. 9.3% for C_3 explorations). This is highlighted by an interaction effect of PMSon*Topography [$F(4, 68) = 5.09,\ p < 0.005$] with a significant difference between *IOI* C_3 and the other conditions. Noise level had no significant impact on false detections, despite the trend observed on *P*-related estimations in Fig. 3(b).

Globally, all three PMSons were equivalent in terms of maximum position estimation accuracy: an average estimation error of $5.8 \pm 5.2°$ (equivalent to 3.4 ± 3.0 mm on the tablet) was observed, merging both true and false detections. For false detections, the error was calculated using the targeted maximum as a reference. A higher estimation accuracy was observed for topography C_3 (means of $4.7 \pm 4.1°$ compared to $6.5 \pm 5.5°$ for both C_1 and C_2), potentially related to the steeper curve of its main maximum

Table 3
Results of the 3-way repeated measures ANOVA performed the evaluation metrics with the PMSon, the Noise, and the Topography as within subjects factors (3 levels each). Evaluation metrics concern the task execution time of phase 1 and 2 (resp. Time 1 and Time 2), False detection of the main maximum in phase 1, Accuracy of the estimated maximum position, and the Correlation between subjects drawings and the original topographies. The notations $F = F(2,34)$ and $F_2 = F(2,32)$ have been adopted for the *F* statistics. The reduction of 2 in degrees of freedom from *F* to F_2 is due to the fact that subjects expertise (2 levels) was identified as a significant factor in phase 2, but not phase 1, and was therefore disregarded in subsequent phase 1 statistical analysis. Results in sub-tables concern pairwise post hoc comparisons (based on Newman–Keuls tests), reported only for significant ANOVAs. $\varepsilon = 0.001$, *p*-value threshold of 5%.

	Time 1		False detection		Accuracy		Time 2		Correlation	
PMSon	F=15.09, p<ε		F=3.58, p=.039		F=1.93, p=.160		F_2=8.78, p<ε		F_2=6.77, p=.003	
	PA	*IOI*	*PA*	*IOI*	*PA*	*IOI*	*PA*	*IOI*	*PA*	*IOI*
P	p<ε	.196	.037	.486	-	-	p<ε	.227	.545	p<ε
PA		p<ε		.069		-		.007		.002
Noise	F=17.03, p<ε		F=0.66, p=.52		F=12.45, p<ε		F_2=8.40, p<ε		F_2=1.94, p=.160	
	N_1	N_2	N_1	N_2	N_1	N_2	N_1	N_2	N_1	N_2
N_0	.002	p<ε	-	-	.010	p<ε	.937	p<ε	-	-
N_1		.015		-		.030		.003		-
Topography	F=15.97, p<ε		F=15.97, p<ε		F=26.80, p<ε		F_2=0.22, p=.805		F_2=60.82, p<ε	
	C_2	C_3	C_2	C_3	C_2	C_3	C_2	C_3	C_2	C_3
C_1	.558	p<ε	1	p<ε	.144	p<ε	-	-	.066	p<ε
C_2		p<ε		p<ε		p<ε		-		p<ε

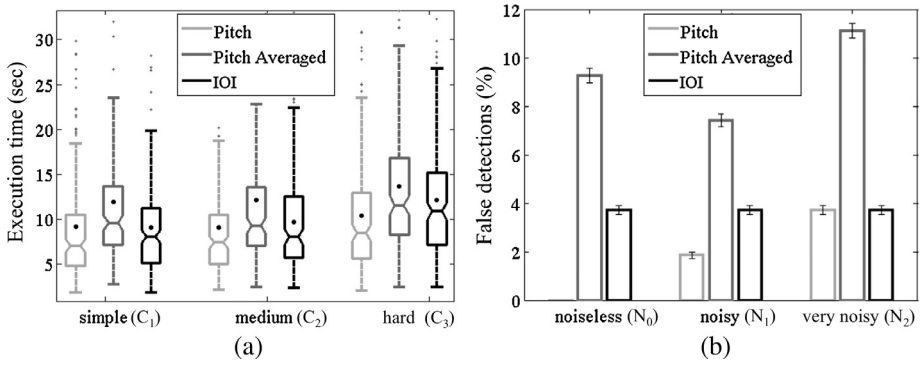

Fig. 3. Results of phase 1 of the experiment. (a) Task execution time (in s) as a function of PMSon and topography difficulty across subjects and noise levels. Black (•) indicates means. (b) Percentage of false detections as a function of PMSon and noise level across subjects for the third topography (C_3, hard). A false detection refers to subjects identifying a secondary maximum as the global maximum.

compared to C_1 and C_2. The presence of noise in the data impacted the estimation accuracy, from $5.1 \pm 7.3°$ (for N_0) to $6.6 \pm 9.0°$ (for N_2) with a significant difference between each noise condition. The analysis of PMSon*Noise level interaction highlights a stronger dependence of *P*itch PMS to noise level than the two other PMS [$F(4, 68) = 3.38,\ p < 0.05$]. Indeed, in the noiseless condition (N_0), *P* led to the highest estimation accuracy whereas it led to the worst estimation accuracy in the very noisy condition (N_2).

The topography shift introduced in Section 5.2 was of no consequence regarding task execution time, false detection or estimation accuracy. The six experts were neither significantly more accurate nor faster than the average, while four of them systematically identified the true maximum across every noise, topography and PMSon conditions.

6.2. Phase 2: Explore, analyze and redraw topographies

Phase 2 concerned subjects' ability to explore and reproduce (draw) data topographies across the different PMSons, noise levels, and topography difficulties. Results extracted from subjects' drawings concern the number of maxima identified in each trial and the correlation value between original and drawn topographies.

Regardless of the PMSon, subjects systematically identified the presence of the global maximum for every topography, as shown in Fig. 4(a). Secondary maxima were more frequently overlooked as their values decreased, particularly for the *IOI* condition. While equal in height, C_3–m_2 was more often neglected than C_2–m_1, particularly in the *IOI* condition. The noise level had no significant impact on the number of identified maxima.

Correlations between drawings and original topographies decreased as the topography grew more complex, significantly so between C_1 and C_2 compared to C_3 as shown in Fig. 4(b) (means of $.93 \pm .04$ and $.86 \pm .08$ respectively). *P* and *PA* based explorations resulted in more precise reproductions of the original topographies compared to *IOI*. Interaction effect of PMSon*Topography highlight a higher dependence of IOI to the topography [$F(4, 68) = 4.47,\ p < 0.005$], particularly for the C_3 condition (related to subjects ignoring the secondary maxima as mentioned above). The noise level had no significant impact on the correlation values.

The impact of PMSons and noise level on phase 2 exploration time did reflect the results of phase 1, significantly shorter with *P* and *IOI* than with *PA* (means of 15.1 ± 15.1 vs. 20.1 ± 18.7 s) and significantly shorter with N_0 and N_1 compared to N_2 (means of 16.1 ± 15.7 vs. 18.2 ± 18.0 s). Surprisingly, the different topography conditions did not have any significant impact on the exploration time.

The topography shift had no significant impact on drawing correlation, number of maxima identified, or exploration time. Drawing correlations and exploration time of expert subjects were significantly higher than non-experts (correlation: [$F(1, 16) = 4.89,\ p = .042$], means of $.92 \pm .07$ vs. $.89 \pm .07$; time phase 2: [$F(1, 16) = 8.11,\ p = .011$], means of 26.0 ± 23.8 vs. 12.1 ± 8.0 s for experts and non-experts respectively). Three out of the six experts identified every single maximum in their drawings, regardless of the PMSon condition. Two of these three expert subjects took on average more than twice as much time than their peers to explore the topography (means of 42.0 and 50.1 s vs.

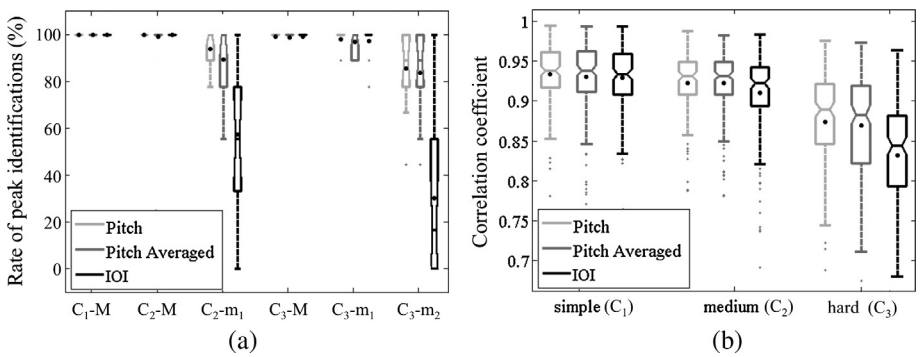

Fig. 4. Results of phase 2 of the experiment. (a) Identification rate of each maximum in the three topographies as a function of PMSon and maximum ID across subjects and noise levels. A maximum was judged as "identified" when it appeared as a bump in subjects drawings. Maxima are labelled "$C_i - M/m_j$", respectively the topography number (i from 1 to 3, i.e. simple to hard) and the maximum ID (e.g. C_3–m_1 is the second maximum of the third topography, c.f. Fig. 2(c)). (b) Evolution of correlation values between subjects' drawings and the original topographies for the different PMSons and topographies across all subjects and noise levels. Black (•) indicates means.

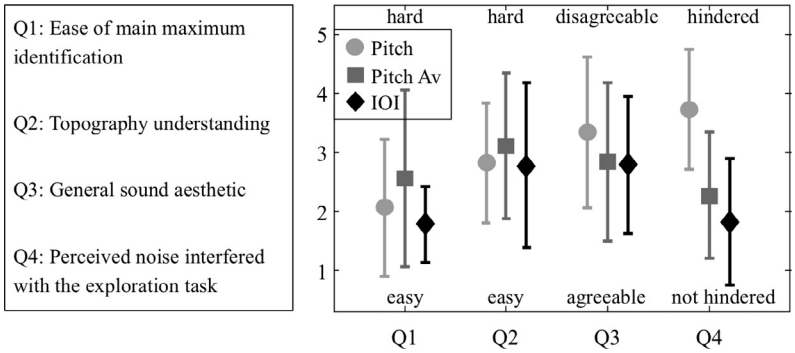

Fig. 5. Post-experiment questions and mean and standard deviation of responses over all subjects.

16.8 s on average). In contrast, the third expert was the second fastest participant (means of 9.6 s).

6.3. Subjective evaluation

Fig. 5 presents subject's responses to the post-experiment questionnaire, completed after each block (i.e. for each PMSon condition). The first two questions were related to phase 1 and 2 respectively. The trend suggests that subjects judged it easier to identify the main maximum and understand the topography in conditions *P* and *IOI* compared to *PA*, yet not significantly so. Questions 3 and 4 concerned the general sound aesthetic and the perceived impact of the noise on the exploration task, where subjects favored *IOI* and *PA* over *P*, significantly for Q4 results $[F(2, 32) = 17.64,\ p < 0.001]$.

When questioned, most subjects reported that the topographies explored with the *IOI* PMSon appeared much simpler (e.g. fewer maxima on average) than those explored with *P* and *PA*. Two of the expert subjects agreed that *IOI* "emphasized" higher local maxima above a certain exploration speed where the simple *P*itch condition *P* systematically induced a mental map of the whole topography. While some subjects preferred *PA* over *P* and *IOI*, the *PA* PMSon was often criticized as "constantly limiting the maximum exploration speed" or "slow and inconsistent" as the presented information depended on the exploration speed.

7. Discussion

The purpose of the present study was to evaluate the capacity of the *IOI* and *PA* PMSons (detailed in Section 4.3) to reduce the instabilities perceived during an interactive auditory graph-based exploration of noisy data. Based on task execution time, estimation accuracy, misinterpretations, etc. the evaluation also questioned the general performance of both *IOI* and *PA* compared to the standard *P*itch PMSon often used in audio-based data exploration.

Subjective evaluations indicated that both *IOI* and *PA* reduced the perception of data instabilities during the exploration, suppressing the aesthetic and fatigue issues related to *P*itch-based exploration. Results otherwise showed that the impact of the noise level on subjects performance did not depend on the PMSon condition.

Quantitative results indicated that subjects handled both localization and exploration tasks (defined in Section 5.3) faster with *P* and *IOI* than with *PA*. As *PA* involved a running average on the data, subjects had to limit their exploration speed to perceive the topography's feature (local minima and maxima) instead of an over-smoothed version of it. Too rapid exploration speeds compared to the averaging period (see Section 4.3.2) are thus assumed to be responsible for the high false detection rate of *PA* compared to *P* and *IOI* during explorations of the most difficult topography C_3.

Table A.4
Average maxima heights reported in subjects' drawings. Heights have been normalized for each drawing between maximum and minimum values drawn on the tablet, ± values give 25th and 75th percentiles. These results indicate a masking effect on the relative amplitude perceived as C_3–m_2, equal in height with C_2–m_1, was perceived as smaller, supposedly related to the presence of C_3–m_1.

Topography-maxID = value	C_2–m_1 = 0.5	C_3–m_1 = 0.8	C_3–m_2 = 0.5
Pitch	0.46 ± 0.16	0.63 ± 0.16	0.40 ± 0.15
Pitch averaged	0.46 ± 0.13	0.61 ± 0.16	0.38 ± 0.14
IOI	0.35 ± 0.15	0.57 ± 0.17	0.27 ± 0.12

Fast exploration with *IOI*, on the other hand, was judged to emphasize the highest values of the topography compared to *P* that systematically induced a mental map of the whole topography. This effect of *IOI* on topography perception is thought to be related to the "adaptive dynamic of estimation" evoked in Section 3, which in essence means that the brain needs less time to evaluate tempi as the *IOI* decreases, and thus notices only the variations related to fast tempi during rapid explorations. The downside of this emphasis is that explorations with *IOI* often led subjects to discard the lowest maxima in the topography, more so in the presence of high valued ones (e.g. C_2–m_1 compared to C_3–m_2 detections in Fig. 4(a). A trend (non-significant) in this figure and in Table A.4 located in A suggests that explorations with *P* and *PA* were also impacted by this "masking effect". Three of the subjects identified as experts (i.e. with some musical background) easily overcame the masking effect, identifying every single maximum regardless of the PMSon condition. While this performance was accompanied by a lengthy and thorough exploration for two of them, the third expert simply reported an ease with tempo estimation due to musical training.

8. Conclusion

This study evaluated the performance of two PMSons designed to reduce the perception of instabilities during the real-time exploration of a noisy data stream. The two PMSons were based on Inter-Onset Interval (*IOI*) and Pitch Averaged (*PA*), i.e. a pitch mapping coupled with a time-based running average. The conducted experiment presented the audio exploration of a 1D topography using a pen tablet as the auditory viewpoint controller, where subjects had to detect the local maxima of a topography for different levels of noise applied to the data. The two PMSons were compared to a standard *P*itch-based sonification in terms of aesthetics, exploration speed, and accuracy.

Subjective evaluations suggested that *IOI* and *PA* reduced the perception of noise-related instabilities in the data compared to

*P*itch. The *IOI* PMSon furthermore preserved the system's reactivity where *PA* over-smoothed topographies' features for fast exploration speeds (compared to the length of the running average). *IOI*'s downside was that it often led subjects to ignore the lowest maxima in topographies that contained high valued ones, subjects being less sensitive to slow rhythmic variations when juxtaposed with rapid ones. The performance of subjects identified as experts indicated that this masking effect could be overcome by training, after which *IOI* achieved *P*itch-like performance and reduction of noise perception during the exploration. Said masking can be exploited for the selective exploration of a topography, naturally focusing listeners on a specific range of data value via the *IOI* sonification mapping.

A side result suggested that, for all three PMSons, the perceived amplitude of a local maximum in the auditory graph changed with the complexity of the underlying topography (further developed in A). This observation would require further investigation through a dedicated study, as it appeared to depend on the sound parameter and may also turn out to be task-specific.

Finally, the results on *P*itch subjective appreciation (low) compared to its objective performance in the exploration task (high) reinforced the findings of previous studies, suggesting that PMSons assessment will generally require both qualitative and quantitative evaluations as raw efficiency and aesthetic considerations do not necessarily point in the same direction.

Acknowledgments

This work was funded in part by the ANRT in the context of a CIFRE industry-linked research funding program with Airbus Defense & Space.

Appendix A. Regarding JND-based PMSon scaling

The assumption on inter-PMSons iso-sensitivity made in Section 4.3 was not verified for the average subject. The variations across PMSons observed in Fig. 4 suggest that the topographies were not perceived with the same level of detail through Pitch and IOI. This result could be seen as a consequence of the masking effect mentioned above, as the three experts who overcame this effect showed equivalent performance in terms of drawing correlation and number of identified maxima for both PMSons.

The assumption on intra-PMSon iso-sensitivity, i.e. a perceptively linear scale for all PMSons due to the JND-based design, was not verified either. Results in Table A.4 show the average values reported for the local maxima in C_2 and C_3 in subjects drawings. While C_2 related results reasonably suggest that subjects perceived this topography without scale distortion, a comparison with C_3 evaluations indicates that the perceptive scale is distorted as the number of local maxima increases. A masking effect similar to the one described for IOI was observed, this time common to all PMSons and related to the perceived amplitude of C_2–m_1 and C_3–m_2. The fact that all three PMSons provided an equivalent accuracy on main maximum position estimation however supports an intra-PMSon iso-sensitivity for the higher topography values.

A subsequent dedicated study would be necessary to clearly assess both iso-sensitivity assumptions for the scaling functions presented in Section 4.3.

References

[1] G. Kramer, Auditory Display: Sonification, Audification, and Auditory Interfaces, Perseus Publishing, 1993.
[2] W.W. Gaver, R.B. Smith, T. O'Shea, Effective sounds in complex systems: the arkola simulation, in: Proceedings of the SIGCHI Conference on Human factors in Computing Systems, ACM, 1991, pp. 85–90.
[3] W.T. Fitch, G. Kramer, Sonifying the body electric: superiority of an auditory over a visual display in a complex, multivariate system, Santa Fe Institute Studies in the Sciences of Complexity-Proceedings, vol. 18, Addison-Wesley Publishing Co, 1994, p. 307.
[4] A.S. Bregman, Auditory Scene Analysis: The Perceptual Organization of Sound, MIT Press, 1994.
[5] T. Hermann, A. Hunt, J.G. Neuhoff, The Sonification Handbook, Logos Verlag, Berlin, 2011.
[6] D.L. Mansur, M.M. Blattner, K.I. Joy, Sound graphs: a numerical data analysis method for the blind, J. Med. Syst. 9 (3) (1985) 163–174.
[7] T. Stockman, L.V. Nickerson, G. Hind, Auditory graphs: a summary of current experience and towards a research agenda, in: Proceedings of the International Conference on Auditory Display, 2005, pp. 420–422.
[8] J.H. Flowers, D.C. Buhman, K.D. Turnage, Data sonification from the desktop: should sound be part of standard data analysis software?, ACM Trans Appl. Percept. 2 (4) (2005) 467–472.
[9] R. Ramloll, W. Yu, S. Brewster, B. Riedel, M. Burton, G. Dimigen, Constructing sonified haptic line graphs for the blind student: first steps, in: Proceedings of the Fourth International ACM Conference on Assistive Technologies, ACM, 2000, pp. 17–25.
[10] B.N. Walker, M.A. Nees, Brief training for performance of a point estimation sonification task, in: Proceedings of the International Conference on Auditory Display, 2005, pp. 6–9.
[11] T.L. Bonebright, M.A. Nees, T.T. Connerley, G.R. McCain, Testing the effectiveness of sonified graphs for education: a programmatic research project, in: Proceedings of the International Conference on Auditory Display, 2001, pp. 62–66.
[12] L.M. Brown, S.A. Brewster, Drawing by ear: interpreting sonified line graphs, in: Proceedings of the International Conference on Auditory Display, 2003, pp. 152–156.
[13] G. Baier, T. Hermann, S. Sahle, U. Stephani, Sonified epileptic rhythms, in: Proceedings of the International Conference on Auditory Display, 2006, pp. 148–151.
[14] F. Grond, J. Berger, Parameter mapping sonification, The Sonification Handbook, 2011, pp. 363–397.
[15] B.N. Walker, G. Kramer, Mappings and metaphors in auditory displays: an experimental assessment, ACM Trans. Appl. Percept. 2 (4) (2005) 407–412.
[16] J.E. Anderson, Sonification Design for Complex Work Domains: Streams, Mappings and Attention Ph.D. thesis, School of Psychology, 2004.
[17] S. Pauletto, A. Hunt, Interactive sonification of complex data, Int. J. Human–Comput. Stud. 67 (11) (2009) 923–933.
[18] J.H. Schuett, R.J. Winton, J.M. Batterman, B.N. Walker, Auditory weather reports: demonstrating listener comprehension of five concurrent variables, in: Proceedings of the 9th Audio Mostly: A Conference on Interaction With Sound, ACM, 2014, p. 17.
[19] G. Parseihian, C. Gondre, M. Aramaki, R. Kronland Martinet, S. Ystad, Comparison and evaluation of sonification strategies for guidance tasks, IEEE Trans. Multimedia 18 (4) (2016).
[20] J.-M. Vézien, B. Ménélas, J. Nelson, L. Picinali, P. Bourdot, M. Ammi, B.F. Katz, J.-M. Burkhardt, L. Pastur, F. Lusseyran, Multisensory VR exploration for computer fluid dynamics in the corsaire project, Virt. Real. 13 (4) (2009) 257–271.
[21] J.L. Reuss, Pulse Oximeter with Signal Sonification, US Patent 6 449 501, September 10 2002.
[22] S. Shelley, M. Alonso, J. Hollowood, M. Pettitt, S. Sharples, D. Hermes, A. Kohlrausch, Interactive sonification of curve shape and curvature data, in: Haptic and Audio Interaction Design, Springer, 2009, pp. 51–60.
[23] B.F. Katz, E. Rio, L. Picinali, O. Warusfel, The effect of spatialization in a data sonification exploration task, in: Proceedings of the International Conference on Auditory Display, 2008, pp. 1–7.
[24] J.H. Flowers, Thirteen Years of Reflection on Auditory Graphing: Promises, Pitfalls, and Potential New Directions, Faculty Publications, Department of Psychology, 2005. pp. 430.
[25] M. Ammi, B.F. Katz, Intermodal audio-haptic metaphor: improvement of target search in abstract environments, Int. J. Human Comput. Interact. 30 (11) (2014) 921–933.
[26] H. Brugger, H.J. Etter, B. Zweifel, P. Mair, M. Hohlrieder, J. Ellerton, F. Elsensohn, J. Boyd, G. Sumann, M. Falk, The impact of avalanche rescue devices on survival, Resuscitation 75 (3) (2007) 476–483.
[27] R. Sarkis, C. Craeye, A. Férréol, P. Morgand, Design of triple band antenna array for GSM/DCS/UMTS handset localization, in: 3rd European Conference on Antennas and Propagation (EuCAP), IEEE, 2009, pp. 3051–3054.
[28] S. Zorn, G. Bozsik, R. Rose, A. Goetz, R. Weigel, A. Koelpin, A power sensor unit for the localization of GSM mobile phones for search and rescue applications, in: IEEE Sensors, 2011, pp. 1301–1304.
[29] D. Poirier-Quinot, B.F. Katz, CAVE-based virtual prototyping of an audio radiogoniometer: ecological validity assessment, in: Proceedings of the International Conference on Auditory Display, 2014, pp. 1–8.
[30] D. Poirier-Quinot, Design of a Radio Direction Finder for Search and Rescue Operations: Estimation, Sonification, and Virtual Prototyping, Thesis, UPMC, May 2015. <https://hal.archives-ouvertes.fr/tel-01182898>.
[31] R.M. Church, W. Meck, A concise introduction to scalar timing theory, in: Functional and Neural Mechanisms of Interval Timing, 2003, pp. 3–22.
[32] J.D. McAuley, Tempo and rhythm, in: Music Perception, Springer, 2010, pp. 165–199.

[33] E.H. Weber, De Pulsu, resorptione, auditu et tactu: Annotationes anatomicae et physiologicae, CF Koehler, 1834.
[34] J. Meinilä, P. Kyösti, T. Jämsä, L. Hentilä, WINNER II channel models, Radio Technologies and Concepts for IMT-Advanced, 2009, pp. 39–92.
[35] B.N. Walker, Magnitude estimation of conceptual data dimensions for use in sonification, J. Exp. Psychol.: Appl. 8 (4) (2002) 211.
[36] Acoustics International Organization for Standardization, Normal Equal-Loudness Level Contours – ISO 226, 2003.
[37] L.M. Brown, S.A. Brewster, S. Ramloll, R. Burton, B. Riedel, Design guidelines for audio presentation of graphs and tables, in: Proceedings of the International Conference on Auditory Display, 2003, pp. 1–5.
[38] S.S. Stevens, J. Volkmann, E.B. Newman, A scale for the measurement of the psychological magnitude pitch, J. Acoust. Soc. Am. 8 (3) (1937) 185–190.
[39] G. Mowbray, J. Gebhard, C. Byham, Sensitivity to changes in the interruption rate of white noise, J. Acoust. Soc. Am. 28 (1) (1956) 106–110.